Available online at www.sciencedirect.com
SCIENCE DIRECT
Journal of Catalysis 239 (2006) 65–73
JOURNAL OF CATALYSIS
www.elsevier.com/locate/jcat

Periodic mesoporous organosilicas with *trans*-(1*R*,2*R*)-diaminocyclohexane in the framework: A potential catalytic material for asymmetric reactions

Dongmei Jiang, Qihua Yang *, Hong Wang, Guiru Zhu, Jie Yang, Can Li *

State Key Laboratory of Catalysis, Dalian Institute of Chemical Physics, Chinese Academy of Sciences, 457 Zhongshan Road, Dalian 116023, China

Received 30 November 2005; revised 17 January 2006; accepted 18 January 2006

Available online 9 February 2006

Abstract

With benzyl group as a linker, *trans*-(1*R*,2*R*)-diaminocyclohexane was incorporated into the framework of mesoporous silica through one-step co-condensation of tetramethoxysilane with N,N′-bis[4-(trimethoxysilyl)benzyl]-(−)-(1*R*,2*R*)-diaminocyclohexane using cetyltrimethylammonium bromide as a structure-directing agent under basic conditions. All materials were fully characterized by X-ray diffraction, N_2 sorption isotherms, transmission electron microscopy, and ^{13}C and ^{29}Si cross-polarization magic-angle spinning nuclear magnetic resonance spectroscopy. Coordinated with $[Rh(cod)Cl]_2$, the material exhibited a TOF up to ∼414 h^{-1} with 30% *ee* for the asymmetric transfer hydrogenation of acetophenone. Various ketones were hydrogenated with different activities and enantioselectivities. An enantioselectivity of about 61% *ee* was observed in the case of 2-acetylnaphthalene. Moreover, a comparison of the catalytic properties of the materials with benzyl and propyl groups as linkers indicates the importance of the rigidity and electron-withdrawing ability of the linker in the high reaction rate of the catalysts.

Keywords: Periodic mesoporous organosilicas; Chirality; Diaminocyclohexane; Asymmetric transfer hydrogenation of ketones

1. Introduction

Asymmetric catalysis is of critical importance in the production of modern pharmaceuticals and agrochemicals. Recently, heterogeneous asymmetric catalysis has attracted much research attention because of the easy recovery and separation of the catalyst from the reaction system. Most of the heterogeneous asymmetric catalysts were synthesized through grafting or immobilization of homogeneous catalyst onto the solid supports [1–7]. There is an increasing demand for the design and synthesis of novel chiral solid materials for the heterogeneous asymmetric catalysis.

trans-1,2-Diaminocyclohexane is among the most commonly used chiral ligands [8]. Its derivatives have been incorporated into the network of amorphous silica through hydrolysis and condensation of organo-bistrialkoxysilanes [9–12]. These silica-based amorphous materials (coordinated with rhodium complex) exhibit low reaction rate (with reactions usually performed for several days) for the asymmetric transfer hydrogenation of ketones because of their low surface areas and small pore volumes. The synthesis of mesoporous materials functionalized with chiral ligands is highly desired. Recently, it was reported that periodic mesoporous organosilicas (PMOs) can be synthesized using $(R'O)_3Si–R–Si(OR')_3$ as precursors in the presence of surfactant under either basic or acidic conditions [13–15]. However, the organic molecules bridged in the framework of most reported PMOs, including methylene, ethylene, phenylene, biphenylene, thiophene, ferrocene, and cyclic CH_2, are nonchiral [16,17]. Very few examples of PMOs with chiral ligands in the framework have been reported [18–20]. The incorporation of chiral ligands into the framework of mesoporous materials will make the materials useful for the heterogeneous asymmetric catalysis.

Recently, we reported the synthesis and catalytic activity of mesoporous organosilicas with ethane bridged in the wall and *trans*-(1*R*,2*R*)-diaminocyclohexane (linked by propyl group) protruding into the channel [21]. After coordination to $[Rh(cod)Cl]_2$, the PMOs can effectively catalyze the transfer hydrogenation of acetophenone; however, they do not exhibit

* Corresponding author. Fax: +86 411 84694447.
E-mail addresses: yangqh@dicp.ac.cn (Q. Yang), canli@dicp.ac.cn (C. Li).

0021-9517/$ – see front matter
doi:10.1016/j.jcat.2006.01.018

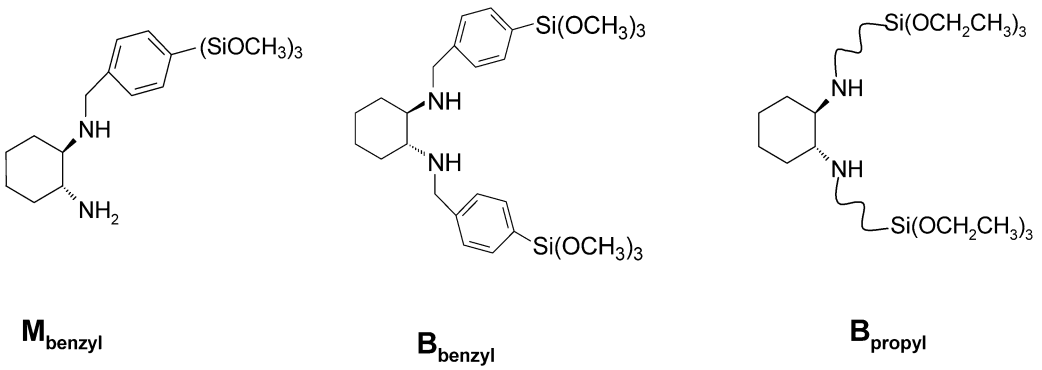

$\mathbf{M}_{benzyl}$ $\mathbf{B}_{benzyl}$ $\mathbf{B}_{propyl}$

Scheme 1. Molecular structure of the precursors.

desirable catalytic properties in terms of reaction rate and enantioselectivity. Consequently, a new precursor with benzyl group as a linker, N,N′-bis[4-(trimethoxysilyl)benzyl]-(−)-(1*R*,2*R*)-diaminocyclohexane ($\mathbf{B}_{benzyl}$), was designed and synthesized (Scheme 1). For comparison, the precursor ($\mathbf{B}_{propyl}$) using propyl group as a linker was also prepared. The PMOs with *trans*-(1*R*,2*R*)-diaminocyclohexane in the framework were synthesized using $\mathbf{B}_{benzyl}$ or $\mathbf{B}_{propyl}$ as the precursor. It was found that the chiral mesoporous material with benzyl group as a linker (coordinated with $[Rh(cod)Cl]_2$) shows a quite high reaction rate and moderate enantioselectivity in the asymmetric transfer hydrogenation of ketones.

2. Experimental section

2.1. Chemicals

The solvents were of analytical quality and dried by standard methods. Other materials were analytical grade and used as purchased without further purification. (3-Chloropropyl)triethoxysilane (97%), cetyltrimethylammonium bromide (CTAB, 99%), and acetophenone (99%) were purchased from Sigma–Aldrich. 4-(Chloromethyl)phenyltrimethoxysilane (97%) was purchased from Gelest. Tetramethoxysilane (TMOS, >98%), tetraethoxysilane (TEOS, 99%), and other reagents were obtained from Shanghai Chemical Reagent. *trans*-(1*R*,2*R*)-Diaminocyclohexane was obtained by the resolution of a commercially available mixture of *cis*- and *trans*-diaminocyclohexane (30/70) as described previously [22]. N,N′-bis[4-(triethoxysilyl)propyl]-(−)-(1*R*,2*R*)-diaminocyclohexane ($\mathbf{B}_{propyl}$) was prepared as described previously [9].

2.2. Synthesis procedures

2.2.1. *Synthesis of* N-[4-(*trimethoxysilyl*)*benzyl*]-(−)-(1*R*,2*R*)-*diaminocyclohexane* ($\mathbf{M}_{benzyl}$)

In a Schlenk tube, a solution of 4-(chloromethyl)phenyltrimethoxysilane (9.5 g, 41.5 mmol) in THF (5 mL) was added dropwise at room temperature to 25 mL of THF containing *trans*-(1*R*,2*R*)-diaminocyclohexane (9.5 g, 83 mmol). The reaction mixture was stirred at room temperature for 1 h and then heated under stirring to 40 °C for 24 h. After filtration, THF was pumped off from the filtrate. The residue was extracted with 75 mL of freshly distilled pentane. The solvent was eliminated in vacuo, leaving a yellowish liquid corresponding to $\mathbf{M}_{benzyl}$ (Scheme 1). ^{1}H NMR ($CDCl_3$): δ 0.99–1.11, 1.18–1.29, and 1.86–2.09 (m, 8H, –NH–(CH–(CH_2)$_4$–CH)–NH$_2$), 2.09–2.38 (m, 2H, –NH–(C*H*–(CH$_2$)$_4$–C*H*)–NH$_2$), 3.61(s, 9H, OCH_3), 3.68–3.97 (d, 2H, CH_2Ph), 7.32–7.65 (m, 4H, H$_{arom}$).

2.2.2. *Synthesis of* N,N′-*bis*[4-(*trimethoxysilyl*)*benzyl*]-(−)-(1*R*,2*R*)-*diaminocyclohexane* ($\mathbf{B}_{benzyl}$)

In a Schlenk tube, 6.34 g (19.6 mmol) of $\mathbf{M}_{benzyl}$ was dissolved in THF (25 mL). Then 2.43 g (9.8 mmol) of 4-(chloromethyl)phenyltrimethoxysilane in THF (5 mL) was added dropwise at room temperature to the above solution. The mixture was stirred at room temperature for 1 h and then heated under stirring to 60 °C for 24 h. After filtration, THF was pumped off from the filtrate. The residue was extracted with 75 mL of freshly distilled pentane. The solvent was eliminated in vacuo, leaving a yellow viscous liquid corresponding to $\mathbf{B}_{benzyl}$ (Scheme 1). ^{1}H NMR ($CDCl_3$): δ 1.07–1.09, 1.20–1.25, 1.74, and 2.15 (m, 8H, –NH–(CH–(CH_2)$_4$–CH)–NH–), 2.18–2.33 (m, 2H, –NH–(C*H*–(CH$_2$)–C*H*)–NH–), 3.61 (s, 18H, OCH_3), 3.71–3.95 (d, 4H, CH_2Ph), 7.30–7.69 (m, 8H, H$_{arom}$). ^{13}C NMR ($CDCl_3$): δ 25.27 (–NH–(CH–CH$_2$–(*C*H$_2$)$_2$–CH$_2$–CH)–NH–), 31.74 (–NH–(CH–*C*H$_2$–(CH$_2$)$_2$–*C*H$_2$–CH)–NH–), 51.09 (O*C*H$_3$), 51.36 (–NH–(*C*H–CH$_2$–(CH$_2$)$_2$–CH$_2$–*C*H)–NH–), 61.61 (–*C*H$_2$Ph), 126.09, 127.69, 128.59, 135.75 (C$_{arom}$).

2.2.3. *Synthesis of the mesoporous silicas with trans-*(1*R*,2*R*)*-diaminocyclohexane in the framework using the benzyl group as a linker* (TB_{benzyl}-*n*-N)

For a typical synthesis, CTAB (0.44 g), $NH_3 \cdot H_2O$ (25 wt%, 5.45 g), EtOH (3.0 g), and deionized water (20.5 g) were mixed at 20 °C under stirring. A mixture of TMOS and $\mathbf{B}_{benzyl}$ (10 mmol of Si) in ethanol (1.6 g) was added to the above solution. The reaction mixture was stirred at 20 °C for 12 h and then heated at 60 °C under stirring for 4 days. After filtration, the powder product was washed thoroughly with deionized water and dried under vacuum at 60 °C. The surfactant was extracted by stirring 1 g of as-synthesized material in 200 mL of ethanol containing 12 M HCl (1.5 g) at 70 °C for 7 h. The products containing protonated *trans*-(1*R*,2*R*)-

diaminocyclohexane were stirred in 0.1 M tetramethylammonium hydroxide aqueous solution for 30 min at room temperature to obtain the free base. After filtration, the powder product was washed with copious amounts of water and ethanol, then dried under vacuum at 60 °C. The materials are denoted as TB_{benzyl}-*n*-N, whereas *n* ($n = 10$, 20, 30, 40) is the mol% of $2\mathbf{B}_{benzyl}/(2\mathbf{B}_{benzyl} + TMOS)$.

2.2.4. Synthesis of the mesoporous silica with *trans*-(1*R*,2*R*)-diaminocyclohexane in the framework using the propyl group as a linker (TB_{propyl}-20-N)

The synthetic method of TB_{propyl}-20-N was similar to that of TB_{benzyl}-20-N, but with TEOS and $\mathbf{B}_{propyl}$ used instead of TMOS and $\mathbf{B}_{benzyl}$, with 20 mol% of $2\mathbf{B}_{propyl}/(2\mathbf{B}_{propyl} + TEOS)$.

2.2.5. Coordination of $[Rh(cod)Cl]_2$ with *trans*-(1*R*,2*R*)-diaminocyclohexane bridged in the mesoporous framework (TB_{benzyl}-*n*-NRh and TB_{propyl}-20-NRh)

In a Schlenk tube, $[Rh(cod)Cl]_2$ in 15 mL of dry ethanol was added to TB_{benzyl}-*n*-N or TB_{propyl}-20-N with the mole ratio of *trans*-(1*R*,2*R*)-diaminocyclohexane:$[Rh(cod)Cl]_2 = 1{:}0.75$. After stirring for 48 h under argon atmosphere at room temperature, a yellow powder product was obtained. The powder was filtered and washed with THF to eliminate the free rhodium complex, then dried under vacuum. The samples are denoted as TB_{benzyl}-*n*-NRh or TB_{propyl}-20-NRh.

2.3. Characterization

Powder X-ray diffraction (XRD) patterns were recorded on a Rigaku D/Max 3400 powder diffraction system using Cu-K_α radiation (40 kV and 30 mA). Transmission electron microscopy (TEM) was done using a JEM-2010 at an acceleration voltage of 120 kV. Nitrogen sorption isotherms were measured at 77 K on an ASAP 2000 system in a static measurement mode. The sample was outgassed at 373 K before the measurement. Pore diameter was calculated from the desorption branch of the isotherm using the BJH method. Solid-state ^{13}C (100.5 MHz) and ^{29}Si (79.4 MHz) CP-MAS NMR were obtained on a Bruker DRX-400 spectrometer with the following experimental parameters: for ^{13}C CP-MAS NMR experiments, 8-kHz spin rate, 3-s pulse delay, 4-min contact time, and 1000 scans; for ^{29}Si CP-MAS NMR experiments, 8-kHz spin rate, 3-s pulse delay, 10-min contact time, and 1000 scans. Tetramethylsilane was used as a reference. N and Rh elemental analyses were done on an Elementar Vario EL III and a Plasma-spec-II (Leeman Laboratories), respectively. Diffuse reflectance UV–vis spectra were collected on a JASCO V-550 UV–vis spectrophotometer using $BaSO_4$ as the reference.

2.4. Catalytic reaction

Asymmetric transfer hydrogenation of ketones was carried out under argon atmosphere. The rhodium-containing mesoporous material (7.36 μmol Rh) in a 50-mL flask was degassed for 1 h at room temperature, followed by the addition of freshly distilled isopropanol (12 mL) and *i*-PrOK (0.1 mmol). The suspension was stirred for 1 h at room temperature, and then ketone (2 mmol) was added with a syringe. The reaction mixture was stirred at 83 ± 2 °C for a specified time under argon atmosphere. The catalytic activity and enantiomeric excess (*ee*) were measured on an Agilent 6890 gas chromatograph equipped with a flame ionization detector and an HP-Chiral 19091G-B213 capillary column (30 m × 0.32 mm × 0.25 μm).

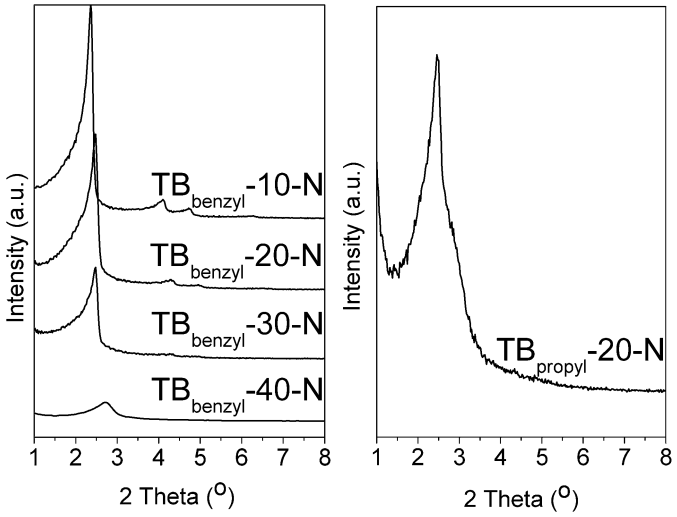

Fig. 1. Powder XRD patterns of TB_{benzyl}-*n*-N [*n* is the mole percent of $2\mathbf{B}_{benzyl}/(2\mathbf{B}_{benzyl} + TMOS)$] and TB_{propyl}-20-N [20 is the mole percent of $2\mathbf{B}_{propyl}/(2\mathbf{B}_{propyl} + TEOS)$].

3. Results and discussion

3.1. Structural characterization of the mesoporous materials with *trans*-(1*R*,2*R*)-diaminocyclohexane in the framework

The mesoporous organosilicas with chiral ligands in the framework were prepared using a direct co-condensation method through the surfactant-assembling pathway. XRD patterns of TB_{benzyl}-*n*-N are presented in Fig. 1. The XRD patterns of TB_{benzyl}-*n*-N ($n = 10$, 20) exhibit three well-resolved diffraction peaks (d_{100}, d_{110} and d_{200}), which can be assigned to the well-ordered two-dimensional hexagonal structure. TB_{benzyl}-30-N displays a sharp d_{100} diffraction peak and a weak d_{110} diffraction peak, whereas TB_{benzyl}-40-N exhibits a broad diffraction peak. The intensity of d_{100} decreases with the amount of $\mathbf{B}_{benzyl}$ in the initial gel mixture, indicating that the mesostructural order of the materials is decreased. A gradual decrease of the d_{100} spacing from TB_{benzyl}-10-N to TB_{benzyl}-40-N is also observed, possibly due to the strong interaction between the organic groups and the tails of the surfactant molecules [23]. The interaction between the organic groups and the tails of the surfactants becomes stronger with increasing amounts of organic groups in the initial gel mixture. The organic groups can be pulled further into the surfactant micelles by the stronger interaction, leading to the decrease in the d_{100} spacing. These results imply that larger amounts of organic groups were incorporated into the mesoporous framework from TB_{benzyl}-10-N to TB_{benzyl}-40-N.

Nitrogen adsorption–desorption isotherms of TB_{benzyl}-n-N are shown in Fig. 2. TB_{benzyl}-n-N ($n = 10, 20, 30$) shows a typical type IV isotherm, which is characteristic of mesoporous material with an ordered arrangement of cylindrical pores. The capillary condensation step is less developed for the materials with higher amounts of organic groups. TB_{benzyl}-40-N exhibits a type I isotherm, indicating that TB_{benzyl}-40-N has a microporous structure. It is noteworthy that an additional uncommon type-H_4 hysteresis loop at P/P_0 above 0.4 is observed for TB_{benzyl}-30-N. The existence of this type-H_4 hysteresis loop may indicate that some structural defects are formed in the hexagonal channel matrix of TB_{benzyl}-30-N [24,25]. The TEM image further clarifies that void defects are irregularly dispersed throughout the ordered pore wall of TB_{benzyl}-30-N, whereas no void defects are observed in other samples, including TB_{benzyl}-10-N (Fig. 3). The presence of void defects in the mesostructured framework of TB_{benzyl}-30-N can explain the uncommon hysteresis loops seen in the N_2 sorption isotherms [24,25]. In our previous work on thioether-functionalized PMOs, we also found that void defects can be formed on the materials when the amount of organic precursor in the initial gel mixture is in the range of certain values [26]. The existence of void defects in TB_{benzyl}-30-N will facilitate diffusion of the guest molecules through the nanochannels of the mesoporous material [27,28].

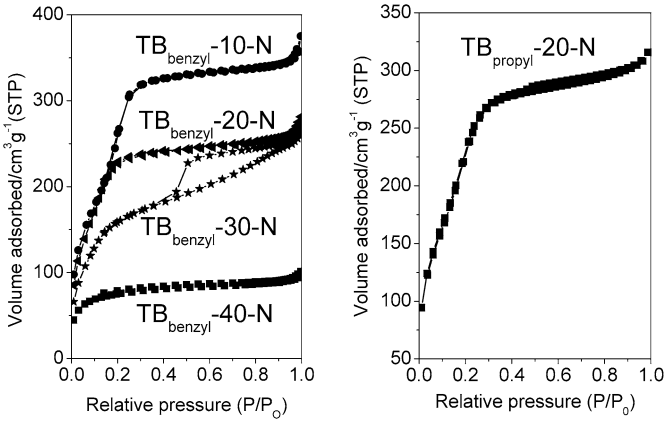

Fig. 2. Nitrogen adsorption–desorption isotherms of TB_{benzyl}-n-N [n is the mole percent of $2\mathbf{B}_{benzyl}/(2\mathbf{B}_{benzyl} + TMOS)$] and TB_{propyl}-20-N [20 is the mole percent of $2\mathbf{B}_{propyl}/(2\mathbf{B}_{propyl} + TEOS)$].

The BET surface area and pore volume decrease gradually from TB_{benzyl}-10-N to TB_{benzyl}-30-N (Table 1). TB_{benzyl}-40-N has the lowest BET surface area, pore volume, and pore diameter among the materials studied.

TB_{propyl}-20-N with propyl group as a linker was synthesized similarly to TB_{benzyl}-n-N by co-condensation of TEOS with $\mathbf{B}_{propyl}$ under basic conditions. A sharp d_{100} diffraction peak is observed in the XRD pattern of TB_{propyl}-20-N, suggesting that the material has an ordered mesoporous structure (Fig. 1). TB_{propyl}-20-N and TB_{benzyl}-10-N have comparable surface areas, pore diameters, pore volumes, and wall thicknesses (Table 1 and Fig. 2).

3.2. Compositional analysis of the mesoporous materials with *trans*-(1*R*,2*R*)-diaminocyclohexane in the framework

The integrity of the organic group in the mesoporous material was identified by ^{13}C CP-MAS NMR spectroscopy. For TB_{benzyl}-10-N, the ^{13}C CP-MAS NMR spectrum (Fig. 4) displays signals corresponding to cyclic CH_2 at 25.2 and 29.8 ppm [11]. The signals centered at 53.7 and 59.8 ppm can be assigned to N*C*H and N*C*H_2, respectively [11]. The existence of the phenyl group is identified by the signals at 128.3, 134.6, and 141.6 ppm [11]. For TB_{propyl}-20-N, the ^{13}C CP-MAS NMR spectrum clearly shows the signals corresponding to cyclic CH_2 and the inner carbon atom of n-propyl groups in the range of 20.0–29.8 ppm and N*C*H/N*C*H_2 in the range of 50.0–60.5 ppm. The sharp signal at 9.9 ppm is ascribed to the carbon atom bonded to silicon [21]. In the ^{13}C CP-MAS NMR spectrum of TB_{propyl}-20-N, the absence of a chemical shift at 67–69 ppm confirms that the surfactant is removed almost completely using the EtOH–HCl extraction method [29].

^{29}Si CP–MAS NMR provides direct evidence for the presence of organic moieties as a part of the silica wall of the mesoporous materials (Fig. 5). For TB_{benzyl}-10-N, and TB_{propyl}-20-N, the signals at about −110 and −100 ppm can be assigned to Q^4 [$Si(OSi)_4$] and Q^3 [$Si(OSi)_3(OH)$] silicon species, respectively. The signals in the range of −50 to −80 ppm are from silicon species (T sites) bridged by the organic group. The existence of T sites confirms that the organic moiety is covalently bonded to the inorganic silicate framework. The ^{13}C and ^{29}Si

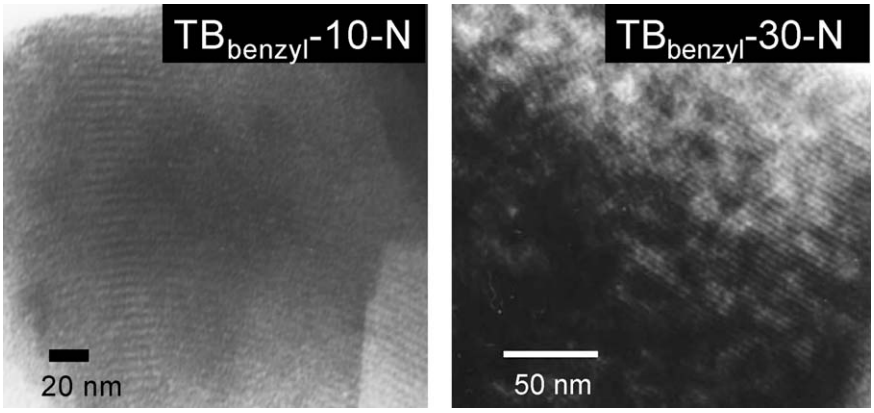

Fig. 3. TEM images of TB_{benzyl}-10-N and TB_{benzyl}-30-N [n is the mole percent of $2\mathbf{B}_{benzyl}/(2\mathbf{B}_{benzyl} + TMOS)$].

Table 1
Physico-chemical data for the mesoporous silicas with *trans*-(1*R*,2*R*)-diaminocyclohexane in the framework

Sample	*d* spacing (nm)	BET surface area (m^2/g)	Pore volume[a] (cm^3/g)	Pore diameter (nm)	a_0[b] (nm)	Wall thickness[c] (nm)
TB_{benzyl}-10-N	3.8	1071	0.55	2.3	4.3	2.2
TB_{benzyl}-20-N	3.5	908	0.42	2.0	4.0	2.0
TB_{benzyl}-30-N	3.6	604	0.40	2.1	4.2	2.1
TB_{benzyl}-40-N	3.2	260	0.15	< 2	3.7	–
TB_{propyl}-20-N	3.7	910	0.53	2.4	4.3	1.9

[a] Total pore volume obtained from the volume of N_2 adsorbed at $P/P_0 = 0.99$.
[b] a_0 is the lattice parameter, $a_0 = 2d_{100}/\sqrt{3}$.
[c] Wall thickness = a_0 − pore diameter.

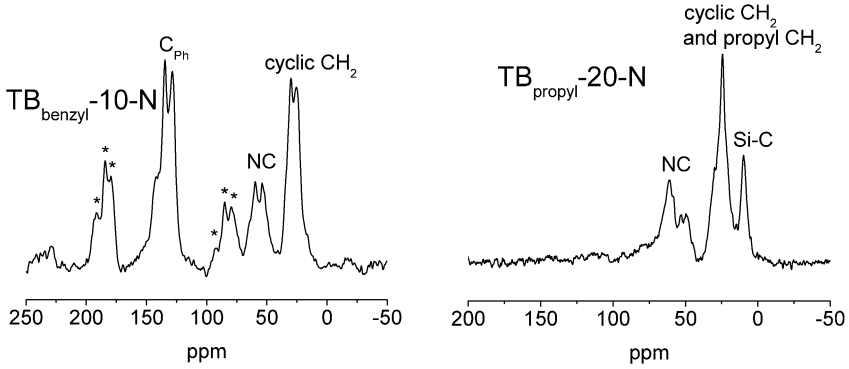

Fig. 4. Solid state ^{13}C CP-MAS NMR spectra of TB_{benzyl}-10-N [10 is the mole percent of $2\mathbf{B}_{benzyl}/(2\mathbf{B}_{benzyl} + TMOS)$] and TB_{propyl}-20-N [20 is the mole percent of $2\mathbf{B}_{propyl}/(2\mathbf{B}_{propyl} + TEOS)$].

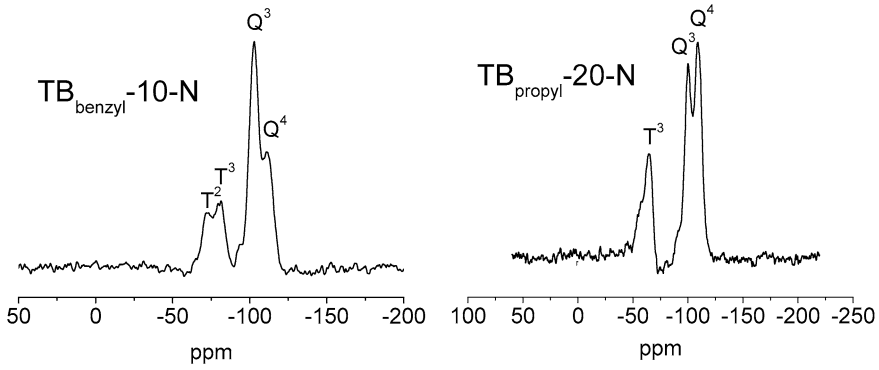

Fig. 5. Solid state ^{29}Si CP-MAS NMR spectra of TB_{benzyl}-10-N [10 is the mole percent of $2\mathbf{B}_{benzyl}/(2\mathbf{B}_{benzyl} + TMOS)$] and TB_{propyl}-20-N [20 is the mole percent of $2\mathbf{B}_{propyl}/(2\mathbf{B}_{propyl} + TEOS)$].

CP-MAS NMR spectra demonstrate that the *trans*-(1*R*,2*R*)-diaminocyclohexane moiety is successfully incorporated in the framework of mesoporous silica.

The content of chiral ligand in the materials was calculated from N elemental analysis (Table 2). With increasing amounts of $\mathbf{B}_{benzyl}$ in the initial gel mixture, more $\mathbf{B}_{benzyl}$ can be incorporated into the mesoporous silica. According to the theoretical estimation, ∼65 to ∼73 mol% of $\mathbf{B}_{benzyl}$ or $\mathbf{B}_{propyl}$ in the initial gel mixture could be incorporated into the mesoporous silicas.

3.3. Catalytic properties of the mesoporous organosilicas coordinated to $[Rh(cod)Cl]_2$

The catalysts were prepared by complexing TB_{benzyl}-*n*-N or TB_{propyl}-20-N with $[Rh(cod)Cl]_2$. The coordination of rhodium complex with *trans*-(1*R*,2*R*)-diaminocyclohexane was characterized by diffuse-reflectance UV–vis spectroscopy (Fig. 6). TB_{benzyl}-20-N shows two sharp peaks in the range of 200–250 nm originating from the phenyl group in the material. Complexing with $[Rh(cod)Cl]_2$, TB_{benzyl}-20-NRh exhibits a new peak at 380 nm. A peak at 230 nm along with a shoulder peak in the range of 300–400 nm is observed in the UV–vis spectrum of TB_{propyl}-20-N. For the material complexed with $[Rh(cod)Cl]_2$, the shoulder peak at 300–400 nm disappears, and a new peak appears at 380 nm. These findings confirm that the rhodium complex coordinates with *trans*-(1*R*,2*R*)-diaminocyclohexane in the materials [11].

3.3.1. Comparison of the catalytic performance of different mesoporous materials coordinated with $[Rh(cod)Cl]_2$

Table 2 lists the Rh content and Rh/chiral ligand ratio for all of the catalysts studied. The Rh/chiral ligand ratio is a direct indication of how much chiral ligand could be coordinated by the

Table 2
The catalytic results of asymmetric transfer hydrogenation of acetophenone

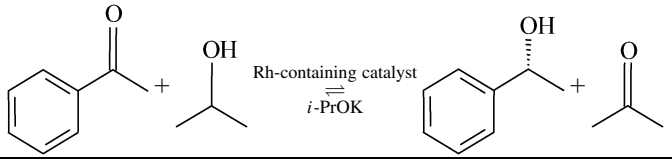

Catalyst	Chiral ligand[a] (mmol/g)	Rh (mmol/g)	Rh/chiral ligand (%)	Conversion[b] (%)	*ee* (%) (S)	TOF (h^{-1})
TB_{benzyl}-10-NRh	0.45 (0.68)	0.10	22	97	26	414
TB_{benzyl}-20-NRh	0.75 (1.14)	0.29	39	93	27	272
TB_{benzyl}-30-NRh	1.02 (1.48)	0.17	17	96	30	336
TB_{benzyl}-40-NRh	1.21 (1.74)	0.10	8	39	22	106
TB_{propyl}-20-NRh	0.93 (1.28)	0.13	14	16	8	22
TB_{propyl}-20-NRh[c]	0.93 (1.28)	0.13	14	36	8	–
EM-4-NRh[d]	0.38 (1.36)	0.24	63	95	22	–
$\mathbf{B}_{benzyl}$	–	–	–	45	21	–

[a] The quantity of chiral ligand in the solids is calculated from elemental analyses. The value in the parenthesis is the theoretical estimation of chiral ligand in the solids, which is calculated based on the formula $(O_{1.5}SiRSiO_{1.5})_{2/n}(SiO_2)_{(100-n)}$, while R is the chiral ligand and $n = 10, 20, 30, 40$.

[b] Conversion is based on acetophenone. Reaction conditions: catalysts (7.36 μmol Rh), *i*-PrOH (12 mL), *i*-PrOK (0.1 mmol), acetophenone (2 mmol), reaction temperature (83 ± 2 °C), reaction time (3 h). Turnover frequencies (TOF) were determined after 0.5 h.

[c] Reaction time (22 h).

[d] From Ref. [21] and reaction time (22 h).

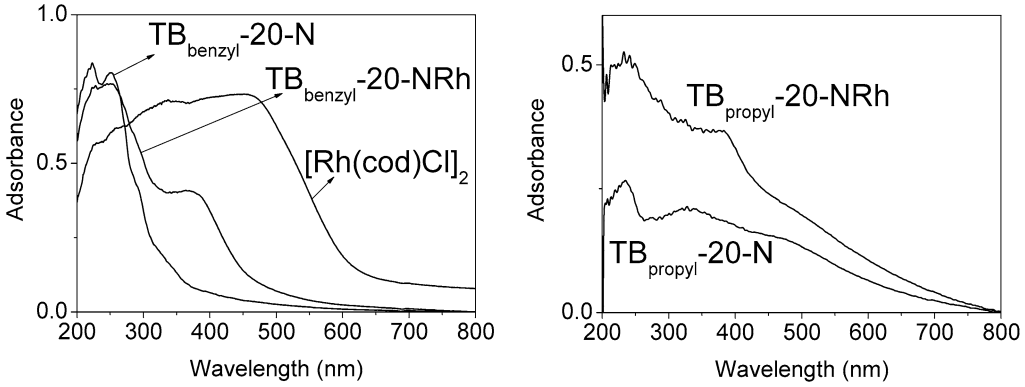

Fig. 6. UV–vis spectra of $[Rh(cod)Cl]_2$ (solid powder), TB_{benzyl}-20-N [20 is the mole percent of $2\mathbf{B}_{benzyl}/(2\mathbf{B}_{benzyl} + TMOS)$] and TB_{propyl}-20-N [20 is the mole percent of $2\mathbf{B}_{propyl}/(2\mathbf{B}_{propyl} + TEOS)$] before and after coordinating with $[Rh(cod)Cl]_2$.

$[Rh(cod)Cl]_2$ complex. The Rh content and Rh/chiral ligand ratio do not increase linearly with incorporation of increasing amounts of chiral ligand into the materials. TB_{propyl}-20-NRh gives a Rh/chiral ligand ratio of 14%, and TB_{benzyl}-20-NRh gives the highest Rh/chiral ligand ratio, 39%. TB_{propyl}-20-NRh and TB_{benzyl}-10-NRh have similar mesoporous structures with comparable BET surface areas, pore diameters, pore volumes, and wall thicknesses (Table 1), but TB_{propyl}-20-NRh has a higher ligand content than TB_{benzyl}-10-NRh. The different Rh/ligand ratios observed for the two kinds of materials is related mainly to the different linkers used for binding the chiral ligand. Because propyl group is softer than benzyl group, *trans*-(1*R*,2*R*)-diaminocyclohexane with propyl group as a linker has more freedom to interact with the hydrophobic chain of the surfactant compared with *trans*-(1*R*,2*R*)-diaminocyclohexane with benzyl group as a linker. Therefore, more chiral ligands are buried in the mesoporous wall in TB_{propyl}-20-N than in TB_{benzyl}-10-N. This leads to lower accessibility of chiral ligands in TB_{propyl}-20-N.

The structural order also has a significant influence on the accessibility of the organic functionality in the mesoporous framework. TB_{benzyl}-10-N and TB_{benzyl}-20-N, with high BET surface areas and pore volumes, display a high Rh/chiral ligand ratio, whereas TB_{benzyl}-30-N, with moderate surface area and pore volume, has a moderate Rh/chiral ligand ratio. TB_{benzyl}-40-N has a very low Rh/chiral ligand ratio (8%), because of its microporous structure. The elemental analysis results indicate that the amount of $[Rh(cod)Cl]_2$ coordinated with the ligands in the mesoporous framework depends on the rigidity of the organic functionality and on the structural order of the materials.

The prepared catalysts were first tested for the asymmetric transfer hydrogenation of acetophenone (Table 2). 2-Phenethyl alcohol is the only product detected. The TB_{propyl}-20-NRh with propyl group as a linker shows a conversion of 16% with only 8% *ee* for 3 h. The conversion is increased to only 36% with the same *ee* by further increasing the reaction time to 22 h. TB_{benzyl}-*n*-NRh ($n = 10, 20, 30$) with benzyl group as a linker exhibits 93–97% conversion with 26–30%

ee. TB_{benzyl}-*n*-NRh ($n = 10, 20, 30$) exhibits much higher activity and *ee* than its homogeneous counterpart (45% conversion with 21% *ee*) and TB_{propyl}-20-NRh. The solid catalyst is superior to the homogeneous catalyst in our case, due mainly to site isolation in the solid catalyst. The lower activity and *ee* of TB_{propyl}-20-NRh compared with TB_{benzyl}-*n*-NRh ($n = 10, 20, 30$) are due in part to the fact that fewer active sites in TB_{propyl}-20-NRh can be accessed by the reactant molecules. This is consistent with the results of elemental analysis. Furthermore, from our previous work [21], we know that EM-4-NRh (*trans*-(1*R*,2*R*)-diaminocyclohexane functionalized mesoporous ethanesilica with propyl group as a linker in the channel) has lower activity and *ee* than TB_{benzyl}-*n*-NRh ($n = 10, 20, 30$) (Table 2). Moreover, EM-4-NRh has a higher Rh/ligand ratio than TB_{benzyl}-*n*-NRh. Therefore, introduction of benzyl group into the N atom of *trans*-(1*R*,2*R*)-diaminocyclohexane contributes mainly to the unique catalytic property of TB_{benzyl}-*n*-NRh.

The foregoing results demonstrate that a linker with spatial rigidity and electron-withdrawing ability is favorable for high catalytic activity and enantioselectivity. The nitrogen atom becomes a stereogenic center after binding to rhodium complex. The chiral microenvironment in the catalysts can be subtly modified by substituting one hydrogen atom with a different organic group on the nitrogen atom in the *trans*-(1*R*,2*R*)-diaminocyclohexane. The subtle modification of the chiral ligand will change the catalytic activity and enantioselectivity of the resulting catalyst. Moreau et al. [11] reported that, compared with alkyl substituents on the nitrogen atom, the bulky benzylic group leads to higher *ee* values, which is consistent with our results.

3.3.2. Relationship between mesoporous structure and catalytic performance

The relationship between the structural properties and catalytic activity of the catalysts can be clearly seen from the time profiles of the catalytic process. Fig. 7 shows the conversion of acetophenone as a function of reaction time catalyzed by TB_{benzyl}-*n*-NRh ($n = 10, 20, 30, 40$). The initial rate of TB_{benzyl}-*n*-NRh is in the following order: TB_{benzyl}-10-NRh ($414\ h^{-1}$) > TB_{benzyl}-30-NRh ($336\ h^{-1}$) > TB_{benzyl}-20-NRh ($272\ h^{-1}$) ≫ TB_{benzyl}-40-NRh ($106\ h^{-1}$) (Table 2). TB_{benzyl}-10-NRh shows the highest initial rate because of its high BET surface area and large pore volume. Interestingly, TB_{benzyl}-30-NRh, with a lower BET surface area, has a faster initial rate than Rh-TB_{benzyl}-20-N. This can be explained by the existence of void defects in TB_{benzyl}-30-N. The void defects amid the mesoporous channels make the reactants diffuse quickly within the porous framework of the catalyst, which compensates for its lower BET surface area and results in a higher reaction rate. TB_{benzyl}-40-NRh shows the lowest initial rate because of its low BET surface area and microporosity. These results again demonstrate the important role of the ordered mesoporous structure in the catalytic performance of the catalyst.

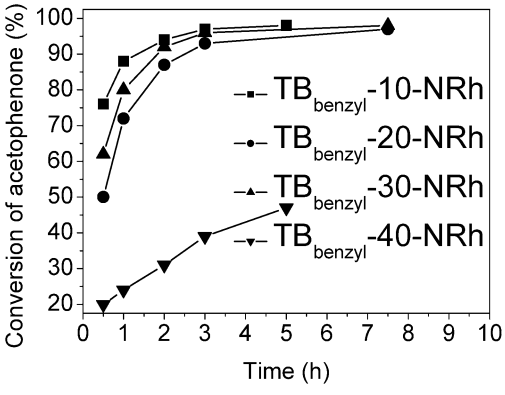

Fig. 7. Asymmetric transfer hydrogenation of acetophenone. Conversion of acetophenone as a function of reaction time on TB_{benzyl}-*n*-NRh [*n* is the mole percent of $2\mathbf{B}_{benzyl}/(2\mathbf{B}_{benzyl} + TMOS)$] catalysts.

3.3.3. Asymmetric transfer hydrogenation of ketones catalyzed by TB_{benzyl}-20-NRh

To investigate the scope of the solid catalysts, asymmetric transfer hydrogenation of a number of different ketones was carried out under identical conditions. The catalytic results are summarized in Table 3. All of the ketones can be converted to their corresponding alcohols on TB_{benzyl}-20-NRh. Acetophenones bearing electron-withdrawing substituents give a faster reaction rate than those with electron-donating substituent, whereas enantioselectivity varies in the range of 18–42%. The conversion of the more crowded 1-acetylnaphthalene and 2-acetylnaphthalene is similar; however, the enantioselectivity is quite different (24% *ee* for 1-acetylnaphthalene and 61% *ee* for 2-acetylnaphthalene). The homogeneous catalyst exhibits similar results, excluding the possibility that pore confinement of the mesoporous materials leads to the different *ee* values for the two reactions. This result indicates that TB_{benzyl}-20-NRh is sensitive to the different reaction substrates, for example, the different substitution position of the ketone functional group on an aromatic ring. The slower reaction rates of 1-acetylnaphthalene and 2-acetylnaphthalene may be due to the difficult diffusion of large molecules in the channel of the mesoporous material.

3.3.4. Hot filtration reaction

To confirm that the catalytic reaction indeed occurs on the solid catalyst, the TB_{benzyl}-30-NRh catalyst was removed from the reaction mixture when the conversion of acetophenone reached 46% (Fig. 8), and then the filtrate was stirred continuously at the same reaction temperature to check whether the homogeneous catalyst (possibly leaching from the solid catalyst) could contribute to the reaction. An additional 6% conversion of acetophenone with the same *ee* value is observed after another 7 h, whereas 96% conversion can be obtained with TB_{benzyl}-30-NRh after 3 h. Rh elemental analysis of the filtrate after reaction showed that ∼1.6% of the Rh in the solid material leached into the solution after the first reaction cycle. (The Rh in the filtration may also come from the nanosized catalyst, which cannot be separated by filtration.) It is obvious that asymmetric transfer hydrogenation of acetophenone is catalyzed mainly by the solid catalyst.

Table 3
Asymmetric transfer hydrogenation of aromatic ketones on TB_{benzyl}-20-NRh

Substrate	Conversion[a] (%)	*ee* (%) (S)
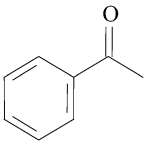	93	27
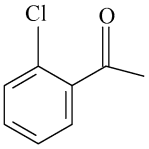	91	42
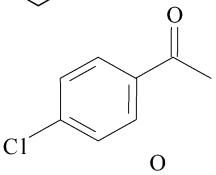	96	18
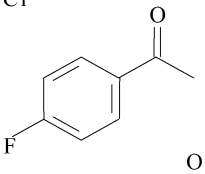	89	23
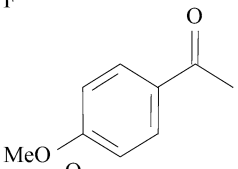	63	20
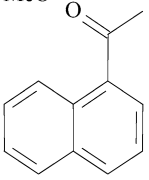	62 (94)	24 (26)
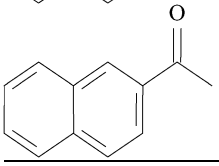	61 (28)	61 (55)

[a] Conversion is based on ketones. Data in the parenthesis is catalyzed by the homogeneous catalyst $\mathbf{B}_{benzyl}$. Reaction conditions: catalysts (7.36 μmol Rh), *i*-PrOH (12 mL), *i*-PrOK (0.1 mmol), ketone (2 mmol), reaction temperature (83 ± 2 °C), reaction time (3 h).

4. Conclusion

Using benzyl group as the linker, the mesoporous organosilicas with *trans*-(1*R*,2*R*)-diaminocyclohexane bridged in the framework were synthesized using a new organo-bistrialkoxysilane N,N′-bis[4-(trimethoxysilyl)benzyl]-(−)-(1*R*,2*R*)-diaminocyclohexane ($\mathbf{B}_{benzyl}$). The mesoporous structure of the final materials largely depends on the amount of the organic functional group in the initial gel mixture. The mesoporous organosilicas with benzyl group as a linker (complexed with $[Rh(cod)Cl]_2$) show remarkably high TOFs of 106–414 h^{-1} with *ee* up to 22–30% for the asymmetric transfer hydrogenation of acetophenone. The linker with spacial rigidity and electron-withdrawing ability is favored over that with high catalytic activity and enantioselectivity. The void defects in the mesoporous channel further improve the reaction rate of the catalyst. The chiral mesoporous material combined with Rh is also an active catalyst for the reduction of a wide range of ketones, with enatioselectivity as high as 61% for the transfer hydrogenation of 2-acetylnaphthalene. These chiral mesoporous organosilicas are potential catalytic materials for asymmetric reactions. The enantioselectivity of these novel mesoporous materials could be further improved through modification of the chiral ligand bridged in the mesoporous framework.

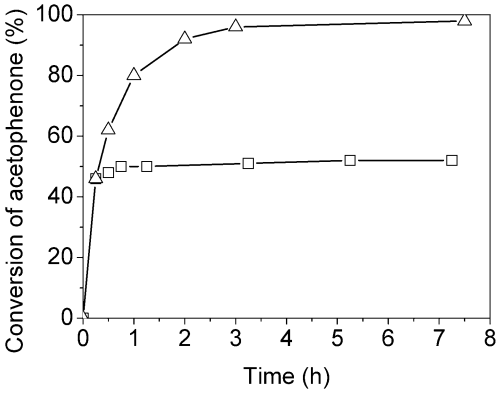

Fig. 8. Asymmetric transfer hydrogenation of acetophenone on the TB_{benzyl}-30-NRh [30 is the mole percent of $2\mathbf{B}_{benzyl}/(2\mathbf{B}_{benzyl} + TMOS)$] catalyst: (△) conversion of acetophenone as a function of reaction time (TB_{benzyl}-30-NRh); (□) conversion of acetophenone as a function of reaction time (TB_{benzyl}-30-NRh was removed after 0.25 h).

Acknowledgments

Financial support for this work was provided by the National Natural Science Foundation of China (grants 20303020, 20321303, and 20503028), the National Basic Research Program of China (grant 2003CB615803), and the Talent Science Program of the Chinese Academy of Sciences.

References

[1] A. Corma, Chem. Rev. 97 (1997) 2373.
[2] B. Thomas, Curr. Opin. Solid State Mater. Sci. 4 (1999) 85.
[3] Q.H. Fan, Y.M. Li, A.C.S. Chan, Chem. Rev. 102 (2002) 3385.
[4] C.E. Song, S.G. Lee, Chem. Rev. 102 (2002) 3495.
[5] P. Hesemann, J.J.E. Moreau, C.R. Chimie 6 (2003) 199.
[6] C. Li, Catal. Rev. Sci. Eng. 46 (2004) 419.
[7] C.E. Song, Ann. Pep. Progr. Chem., Sect. C. 101 (2005) 143.
[8] Y.L. Bennani, S. Hanessian, Chem. Rev. 97 (1997) 3161.
[9] A. Adiam, J.J.E. Moreau, M. Wong Chi Man, Chirality 12 (2000) 411.
[10] A. Adiam, J.J.E. Moreau, M. Wong Chi Man, J. Mater. Chem. 7 (1997) 2331.
[11] A. Brethon, J.J.E. Moreau, M. Wong Chi Man, Tetrahedron: Asymmetry 15 (2004) 495.
[12] C. Bide, D. Gauthier, J.J.E. Moreau, M. Wong Chi Man, J. Sol-Gel. Technol. 20 (2001) 313.
[13] S. Inagaki, S. Guan, Y. Fukushima, T. Ohsuna, O. Terasaki, J. Am. Chem. Soc. 12 (1999) 9611.
[14] B.J. Melde, B.T. Holland, C.F. Blanford, A. Stein, Chem. Mater. 11 (1999) 3302.
[15] T. Asefa, M.J. MacLachlan, N. Coombs, G.A. Ozin, Nature 402 (1999) 867.

[16] W.J. Hunks, G.A. Ozin, J. Mater. Chem. 15 (2005) 3716.
[17] X.Y. Bao, X.S. Zhao, J. Phys. Chem. B. 109 (2005) 10727.
[18] C. Baleião, B. Gigante, D. Das, M. Álvaro, H. Garcia, A. Corma, Chem. Commun. (2003) 1860.
[19] M. Álvaro, M. Benitez, D. Das, B. Ferrer, H. García, Chem. Mater. 16 (2004) 2222.
[20] C. Baleião, B. Gigante, D. Das, M. Álvaro, H. Garcia, A. Corma, J. Catal. 223 (2004) 106.
[21] D.M. Jiang, Q.H. Yang, J. Yang, L. Zhang, G.R. Zhu, W.G. Su, C. Li, Chem. Mater. 17 (2005) 6154.
[22] F.L. Jay, N.J. Eric, J. Org. Chem. 59 (1994) 1939.
[23] M.A. Wahab, I. Imae, Y. Kawakami, C.S. Ha, Chem. Mater. 17 (2005) 2165.
[24] H.P. Lin, S.T. Wong, C.Y. Mou, C.Y. Tang, J. Phys. Chem. B 104 (2000) 8967.
[25] J.L. Zhang, S.R. Zhai, Y. Zhang, D. Wu, Y.H. Sun, Y.X. Yang, L. Chen, F. Deng, Catal. Today 93–95 (2004) 529.
[26] J. Liu, J. Yang, Q.H. Yang, G. Wang, Y. Li, Adv. Funct. Mater. 15 (2005) 1297.
[27] S.A. Bagshaw, E. Prouzet, T.J. Pinnavaia, Science 269 (1995) 1242.
[28] P.T. Tanev, T.J. Pinnavaia, Chem. Mater. 8 (1996) 2068.
[29] M.A. Wahab, I. Kim, C.-S. Ha, J. Solid State Chem. 177 (2004) 3439.